Sādhanā Vol. 33, Part 4, August 2008, pp. 433–441. © Printed in India

A more general model for the analysis of the rock slope stability

MEHDI ZAMANI

Department of Technology and Engineering, Yasouj University, Daneshjoo Avenue, Yasouj, Iran 75914
e-mail: mahdi@mail.yu.ac.ir

MS received 3 August 2007; revised 14 February 2008

Abstract. The slope stability analysis has many applications in the engineering projects such as the dams, the roads and open pits structures. The method of analysis is usually based on the equilibrium conditions of the potential plane and wedge failures. The zone of the potential failure is stable whenever the stability forces dominate instability characteristics of the slope. In most of the classic methods of slope stability analysis, the joint surfaces are assumed to be continuous along the potential failure zone. These can cause an underestimated solution to the analysis. In this research the joint trace length is considered to be discontinuous across the potential surface of failure as it happens in nature. Therefore, there exists a rock bridge between the local joint traces. Because of the numerous problems related to the rock slope stability the above assumption is satisfied and the shear strength characteristics of intact rock have taken part in the analysis. The analysis presented here gives a better concept, view, and idea of understanding the physical nature of rock slopes and includes more parameters governing the stability of the potential failure zone.

Keywords. Wedge failure; slope stability; trace length; joint set; sliding force.

1. Introduction

One of the parameters effecting the slope stability analysis is joint distribution. The analysis of rock slope stability has many applications in the design of rock slopes, roofs and walls of tunnels. Because of the different factors causing joints in rocks, rock heterogeneity and non-uniformity of the forces taking part in joint creation, the joints are not continuous in the scale of engineering projects. Therefore, there exist rock bridges between the local joint surfaces, and the joint surfaces are limited to the intact rocks. In most cases the dimensions of the joints (length, width, etc.) are measurable on the rock outcrops. If the joint surface is the surface of the layering between two geological formations, the assumption of the continuity of the joint surface will be correct.

There are four mechanisms of rock slope instability; circular sliding, plane sliding, wedge sliding and toppling. Whenever the rock mass can be justified as a homogeneous medium

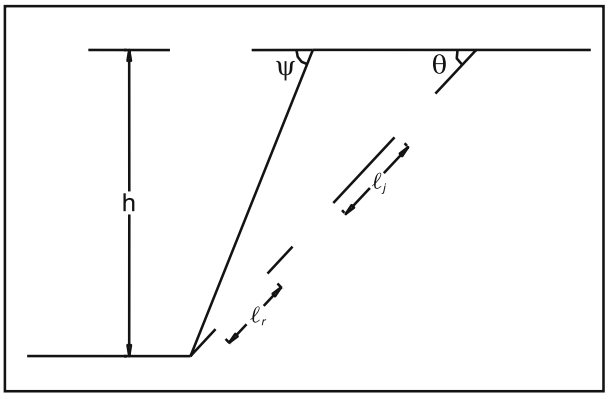

Figure 1. Plane failure in rock slope.

the circular failure can be considered. When the instability is dictated by the presence of pre-existing discontinuities, the instability takes the form of plane sliding, wedge sliding or toppling. A three-dimensional wedge failure analysis was presented by Coates (1967), Lond *et al* (1970) and Hudson & Harrison (1997). Hoek & Bray (1974) explained a solution to the wedge failure problems in which both planes of sliding possess different cohesions and angles of friction, as well as the existence of water in upface tension crack. Goodman (1976) analysed the wedge failure mechanism by using the block theory approach. All the above researchers assumed the continuity of joint surface along its sliding plane in the scale of engineering works. The idea of the rock bridge consideration in instability analysis was mentioned by Abel (1990). He considered the limitness of joint surface and the existence of rock bridge along the sliding surface in the plane failure and wedge failure analysis. Priest (1985) investigated the prediction of unstable block or wedge by the use of stereographic rotation plane.

2. Plane failure analysis

The potentially unstable regions in rock slopes consist of some wedges. The wedges are usually four or five sided. To form a wedge from a solid at least four limiting surfaces (sides) are needed. The sides consist of the joint surfaces, faults, discontinuities, bedding planes and free surfaces. In the plane failure analysis, the wedge slides along one of its limiting sides and the other sides consist of free or open surfaces. In this case the surface area of the plane of sliding is obtained regarding the height of slope. For the sake of simplicity the analysis is done based on the unit thickness of the wedge. Figure 1 shows a vertical section of a wedge due to the potential of sliding. The weight of the wedge is obtained from the following Equations

$$w = h^2/2(\cot q\theta - \cot y\psi)\gamma_r, \ell = h/\sin\theta, \tag{1}$$

where γ_r is the unit weight of rock in KN/m^3, w is the weight of the potential sliding body in KN, ℓ is the length of the sliding surface in meter, ψ is the rock face slope angle, h is the slope height, and θ is the angle of the potential sliding surface. All angles are in degree unit (D). The plane having the potential of sliding consists of two parts ℓ_j and ℓ_r. Part ℓ_j consists of the joint surface length and part ℓ_r is the rock bridge surface length. Therefore, the resistant

property of the sliding surface increases from a minimum of the joint shear strength to a maximum value of the intact rock shear strength. The increasing of ℓ_r causes the increasing of the stability of the rock slope. The factor of safety of the plane failure analysis is obtained from the Eq. (2):

$$FS = T/P = (T_j + T_r)/w \sin\ \theta \tag{2}$$

$$T_j = N \tan(\phi_j + i)(1 - a) + C_j(1 - a)\ell, \quad T_r = N \tan(\phi_r)a + C_r a\ell. \tag{3}$$

The length of the potential sliding surface can be approximated as $\ell = n(\bar{\ell}_j + \bar{\ell}_r) + \alpha\bar{\ell}_j$.

Where n and α are parameters, n is an integer value, and $\alpha \in [0, 1]$. With the substitution of $p = \bar{\ell}_j/\bar{\ell}_r$ in the above equation, it results:

$$\ell = [n(p + 1) + \alpha p]\bar{\ell}_r \tag{4}$$

$$a = \frac{n\bar{\ell}_r}{[n(p + 1) + \alpha p]\bar{\ell}_r} = \frac{n}{n(p + 1) + \alpha p}. \tag{5}$$

For a conservative approach α and n equal to:

$$a = \frac{n}{n(p + 1) + p}, \quad n = \text{integer value of } \left[\frac{\ell}{\bar{\ell}_j + \bar{\ell}_r}\right], \tag{6}$$

where:

$N = w \cos\theta$, $P = w \sin\theta$, $\ell_j = (1 - a)\ell$, and $\ell_r = a\ell$,
T_r = the resistant force governing to the rock bridge (Kilo Newton, KN),
T_j = the resistant force governing to the rock joint surface (KN),
FS = the factor of safety,
T = the resistant forces (KN),
P = the sliding forces (KN),
N = the component of the weight force normal to the sliding plane (KN),
ϕ_j = the friction angle (joint surface),
ϕ_r = the friction angle (intact rock),
i = irregularity angle obtained from stereographic projection of the governing joint set,
C_j, C_r = the cohesion coefficients of the rock joint and rock bridge (KN/m^2), respectively
a = the ratio of the rock bridge area to the sliding area,
$\bar{\ell}_j$ = the average joint trace length (m), and
$\bar{\ell}_r$ = the average rock bridge length (m).

3. Wedge failure analysis

When several joint sets and one or two free surfaces in the rock mass exist, the potential of wedge failure is evident. For rock slopes usually two free surfaces (lower outcrop and upper outcrop) are present, figure 2. The lower surface could have high slope while the upper outcrop surface can be a horizontal surface or a surface with low slope angle. In all the above cases the wedge failure analysis can be applied. The size and the extension of wedge due to sliding is a function of the rock slope dimensions and the tunnel geometric characteristics.

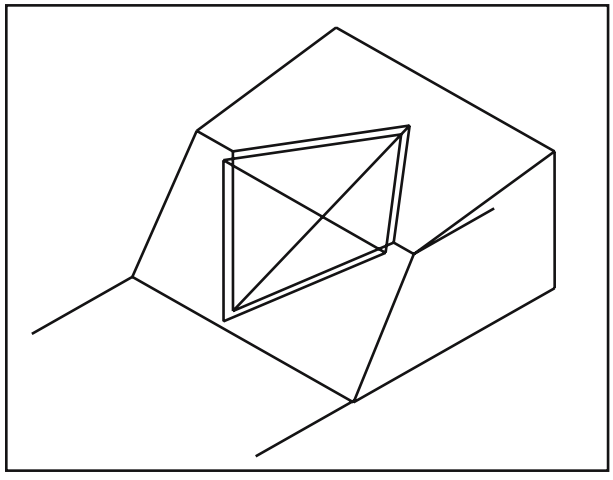

Figure 2. The wedge failure phenomena in a rock slope.

Figure 2 shows the wedge failure phenomena in a rock slope. The wedge failure analysis is based on satisfying the equilibrium conditions of the wedge. If w be the weight of the wedge, the vector w can be divided into two components in the parallel and normal directions to the joint intersection, figure 3.

$$N = w\cos\theta,\ \ P = w\sin\theta \tag{7}$$

The vector N in the figure 3 is divided into two components N_1 and N_2, normal to the joint set surfaces 1 and 2, respectively as follows:

In figure 4 the equilibrium conditions in the directions x and y are as follows:

$$N_{1x} = N_{2x}, \qquad N_{1y} + N_{2y} = N \tag{8}$$

$$N_{1x} = N_1\sin\alpha_1, \qquad N_{2x} = N_2\sin\alpha_2 \tag{9}$$

$$N_{1y} = N_1\cos\alpha_1, \qquad N_{2y} = N_2\cos\alpha_2. \tag{10}$$

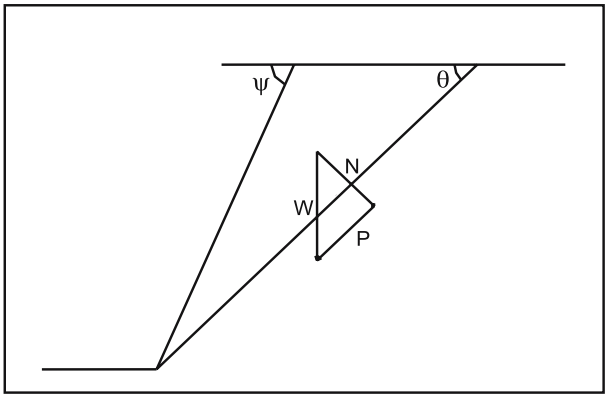

Figure 3. Conditions of effective forces in the wedge failure analysis.

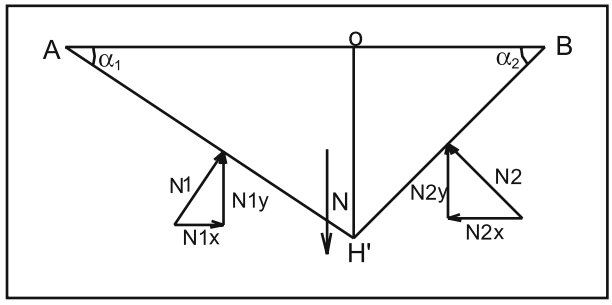

Figure 4. The plane normal to the intersection of joint sets 1 and 2.

The forces N_1 and N_2 can be obtained from the Eqs. (8), (9), and (10) as follows:

$$\begin{cases} N_1 \sin\alpha_1 = N_2 \sin\alpha_2 \\ N_1 \cos\alpha_1 + N_2 \cos\alpha_2 = N = w\cos\theta \end{cases}, \tag{11}$$

where

$$N_1 = \frac{N \sin\alpha_2}{\sin(\alpha_1 + \alpha_2)}, \qquad N_2 = \frac{N \sin\alpha_1}{\sin(\alpha_1 + \alpha_2)}. \tag{12}$$

3.1 *Calculation of the angles α_1 and α_2*

In figure 5 the line CC' is the intersection line of two joint surfaces 1 and 2. The segment OH is drawn vertically in the normal plane passing through the line of intersection CC'. Figure 4 is drawn in the three-dimensional view as the triangle ABH'. From the point O the segment OH' normal to the intersection is drawn. The plane ABH' is the plane normal to the intersection CC' at point H'. From the points H and A on plane 1, two lines are drawn so that the first one is parallel to the strike and the second one is in the direction of dip line.

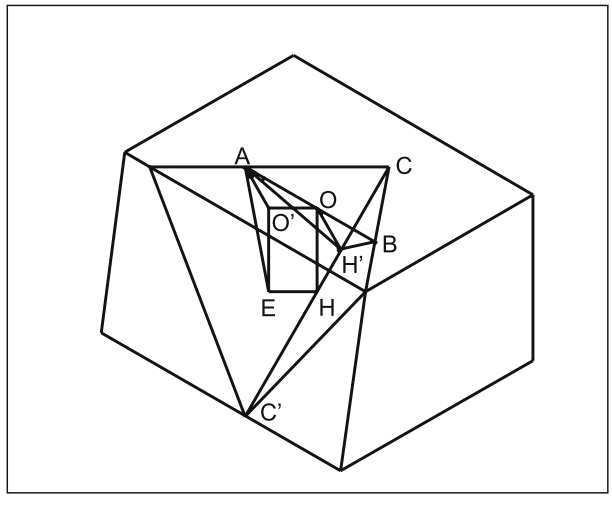

Figure 5. The geometry of the sliding wedge.

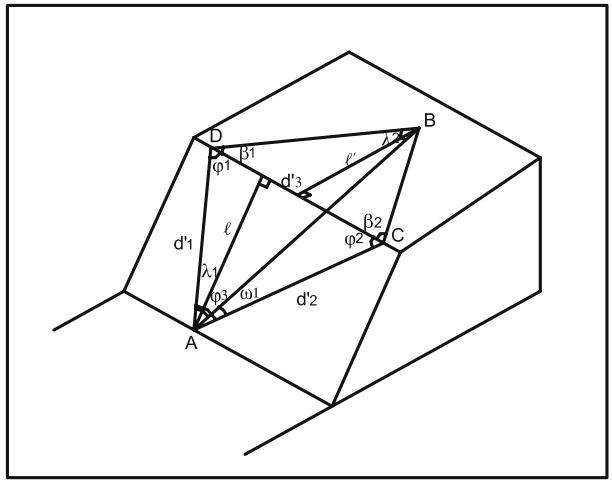

Figure 6. Three-dimensional view of wedge and its parameters.

These two lines intersect at point E. EO' is drawn parallel and with the same size as HO. The quadrilateral OO'EH is rectangle. Using the geometric and trigonometric relationships in the triangles H'OA, OO'A, and O'AE, the angles α_1 and α_2 are obtained from the following Equation.

$$\cos\theta \cos\gamma_1 \tan d_1 = \frac{H'O}{HO} * \frac{AO'}{AO} * \frac{EO'}{AO'} = \frac{H'O}{AO} = \tan\alpha_1, \tag{13}$$

it can be shown in the same way that $\tan\alpha_2 = \cos\theta \cos\gamma_2 \tan d_2$, where $\mathrm{HO} = \mathrm{EO}'$, $\angle\mathrm{EAO}' = \angle d_1$, $\angle\mathrm{OAH}' = \angle\alpha_1$, $\angle\mathrm{OBH}' = \angle\alpha_2$, $\angle\mathrm{HOH}' = \angle\theta$, and $\angle\mathrm{OAO}' = \angle\gamma_1$.

In which d_1 and d_2 are the slope angles of the joint set 1 and 2, respectively. The angles γ_1 and γ_2 are the angles between the dip directions of joint sets 1 and 2 and the strike of the plane normal to intersection line, respectively.

3.2 *Determination of the wedge weight and the area of the sliding surfaces*

The angles and the sides' lengths governing the calculation of the wedge weight and the areas of the sliding surfaces are shown in figure 6. The lengths d_1', d_2', and d_3' are in meters and are obtained from the trigonometric relationships and similarities as shown in the following Equations:

$$d_1' = \frac{h}{\sin\varphi_1 \sin\psi} \tag{14}$$

$$d_2' = \frac{h}{\sin\varphi_2 \sin\psi} \tag{15}$$

$$d_3' = \frac{h}{\sin\psi}(\cot\varphi_1 + \cot\varphi_2) = \frac{(\tan\beta_1 + \tan\beta_2)}{\tan\beta_1 \cdot \tan\beta_2}\ell' \tag{16}$$

$$w = \frac{1}{6} d_3' \ell' h \gamma_r = \frac{\tan\beta_1 \cdot \tan\beta_2}{6(\tan\beta_1 + \tan\beta_2)} d'^2_3 h \gamma_r \tag{17}$$

$$S_1 = \frac{1}{2} d'^2_1 \frac{\sin\lambda_1 \sin\lambda_3}{\sin\lambda_2}, \sin\lambda_3 = \sin(\lambda_1 + \lambda_2) \tag{18}$$

$$S_2 = \frac{1}{2} d'_1 d'_2 \frac{\sin\lambda_3 \sin\omega_1}{\sin\lambda_2}. \tag{19}$$

In which S_1 and S_2 are the areas of the sliding surfaces respect to the joint sets 1 and 2, respectively. The angles φ_1, φ_2, β_1, β_2, λ_1, λ_2 and λ_3 can be obtained by using the governing trigonometric relationships and also by the graphical method using the stereographic projections of the joint sets 1, 2, upper and lower free surfaces as shown in figure 7. For obtaining the ratio of the intact rock to the broken rock, a, a statistical model is applied. In this model it is assumed that all discontinuities are elliptic discs. The rock joint length distribution on outcrop of rock mass can be simulated by the intersection of a random normal plane with a specified ellipse. Also the position of ellipse in the rock mass is random. For this purpose it is considered an ellipse with the major and minor diameters of 3·5 m and 1·7 m, respectively. If this ellipse is intersected by a random normal plane, the intersection lines have a distribution as shown in figure 8. The characteristics of its distribution are in table 1. This distribution could be similar to joint length distribution in some rock masses. The major and minor diameters of ellipse can be estimated directly from the joint length distribution as $\ell_{j\,\max}$ and q_1, where $\ell_{j\,\max}$ is the maximum length of the joint set, and q_1 is the first quartile (percentile of 25%) of the joint length distribution. The area of the joint surface is $S_j = \frac{\pi}{4} q_{1j} \ell_{j\,\max}$. If the joint spacing (rock bridge) distribution in rock masses obeys the distribution of figure 8, the surface of rock bridge equals $S_r = \frac{\pi}{4} q_{1r} q_{3r}$. The value of a is obtained as the ratio of Sr to the $Sr + Sj$, Eq. (20).

$$a = \frac{q_{1r} q_{3r}}{q_{1r} q_{3r} + \ell_{j\,\max} q_{1j}} \tag{20}$$

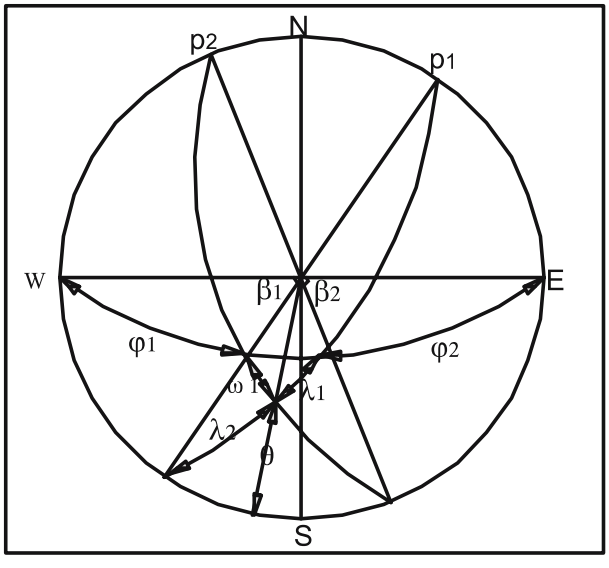

Figure 7. The stereographic projection of the sliding wedge.

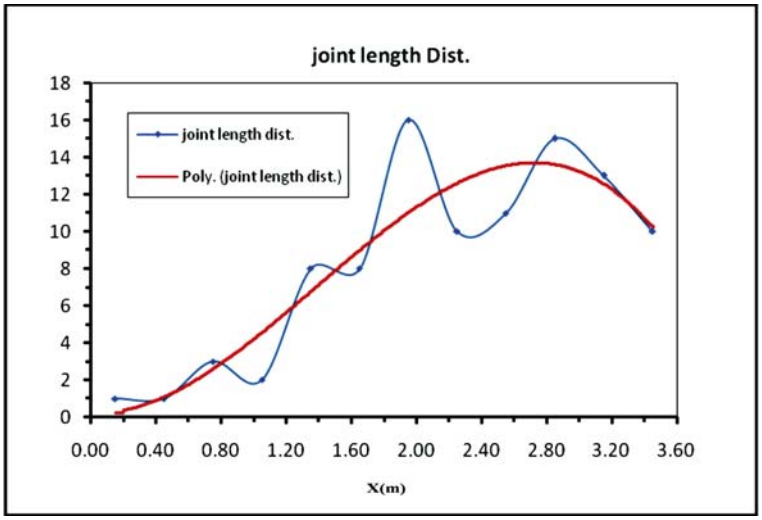

Figure 8. The distribution of the intersection of ellipse with a random normal plane.

where:

q_{1r} = the first quartile (percentile 25%) of the joint spacing distribution,
q_{3r} = the third quartile (percentile 75%) of the joint spacing distribution.

The Eq. (20) can be determined for both joint sets 1 and 2. The factor of safety can be calculated from the Eq. (2) where T_1 and T_2 are obtained from the Eq. (21).

$$\begin{cases} T_1 = N_1 \tan(\phi_{j1} + i_1)(1 - a_1) + C_{j1}(1 - a_1)S_1 + N_1 a_1 \tan\phi_{r1} + C_{r1} a_1 S_1 \\ T_2 = N_2 \tan(\phi_{j2} + i_2)(1 - a_2) + C_{j2}(1 - a_2)S_2 + N_2 a_2 \tan\phi_{r2} + C_{r2} a_2 S_2 \end{cases}, \tag{21}$$

where N_1, N_2 and a_1 are obtained from the Eqs. (12) and (20), respectively. The internal frictions of the intact rock ϕ_{r1} and ϕ_{r2} and the cohesion coefficients of the intact rock C_{r1}

Table 1. The statistical parameters of the intersection distribution.

Parameters	Value (m)
$\ell_{j\,\min}$	0·2
$\ell_{j\,\max}$	3·5
Mean	2·31
Median	2·4
Mode	2·8
σ (S.D.)	0·77
q_1	1·8
q_3	2·9

and C_{r2} are determined from the Triaxial-Compressive tests and using the Mohr–Colomb criterion. The correction factor for the effect of intact rock specimen diameter on the cohesion coefficients could also be included. The internal friction angles of the joint sets 1 and 2 surfaces ϕ_{j1} and ϕ_{j2} are obtained from the Shear-Tests on the polished rock joint specimens. The irregularity angles i_1 and i_2 are determined from the direct measurements on the rock outcrops using the stereographic projections of the joint sets 1 and 2.

4. Conclusions and recommendations

The analysis presented in this study gives more value to the safety factor since it considers more factors and parameters related to the stability of rock slopes. The presented model has the advantage of applying the better natural conditions of the slope stability characteristics compared to other classical methods in this area.

It is suggested that the statistical distributions of joint length and joint spacing are obtained from the governing field data for each joint set. By using these statistical distributions the ratio of intact rock portion to broken rock portion can be obtained more accurately. Also with the investigation of probability density functions of joint length and joint spacing one can predict the geometry and the form of joint surface. The geometry of joint surface shows the amount of effectiveness of joint trace length on unstability of rock slopes. Also it is recommended to solve some practical problems and the obtained factor of safety is compared with the solutions of the classic models.

References

Abel J F 1990 Rock mechanics. Colorado School of Mine, USA

Coates D F 1967 Rock mechanics principles. Canadian Department of Energy, Mines and Resources, Monograph 874

Goodman R E 1976 Methods of geological engineering in discontinuous rocks. St. Paul: West Publisher

Hoek E, Bray J 1974 Rock slope engineering. (London: Institute of Mine. and Metal.)

Hudson J A, Harrison J P 1997 Engineering rock mechanics: An introduction to the principles. (UK: Pergamon)

Londe D, Vigier G, Vormeringer R 1970 Stability of rock slopes: A three-dimensional study. *J. Soil Mechanics and Found. Divi. Proc. Amer. Soc. of Civil Eng.*

Priest S D 1985 Hemispherical projection methods in rock mechanics. (London: George Allen & Unwin)